

## Original Article

## Effects of surface roughness and alloying element on surface morphology and tribology of low-alloy steel after gas-nitrocarburizing

Naruenat Polyiam<sup>1</sup>, Prasert Aengchuan<sup>1\*</sup>, Nipon Taweejun<sup>2</sup>,  
and Piyamon Poapongsakorn<sup>3</sup><sup>1</sup> School of Manufacturing Engineering, Institute of Engineering,  
Suranaree University of Technology, Mueang, Nakhon Ratchasima, 30000 Thailand<sup>2</sup> Thai Tohken Thermo Co.,Ltd, Mueang, Chonburi, 20000 Thailand<sup>3</sup> Mechanical Innovation and Tribology Group, School of Engineering,  
University of Birmingham, Birmingham, United Kingdom

Received: 3 May 2020; Revised: 21 July 2020; Accepted: 8 September 2020

---

**Abstract**

This paper aimed to study the effects of initial surface preparation and Chromium (Cr) content on morphology and tribological properties of gas nitrocarburized AISI 1015 steel and AISI 4115 steel. Two different surface preparation methods, i.e., polishing and machining, were employed in order to achieve different surface roughnesses and topologies. Surface treatment was performed using nitrocarburizing technique. After the surface treatment, white layers formed by gas nitrocarburizing were observed and analyzed by following techniques; surface roughness test, optical microscopy, scanning electron microscopy, X-ray diffraction, microhardness test, and pin-on-disk test. It was found that morphology and tribological properties of the nitrocarburized steels were significantly influenced by the initial surface roughness. The results indicate that the wear volume loss increases with an increase in the initial surface roughness, whereas increasing of Cr element increases the surface hardness of steel, but decreases the wear resistance.

**Keywords:** gas nitrocarburizing, surface roughness, low alloy steel, wear

---

**1. Introduction**

Low alloy steel is extensively used to produce a wide range of mechanical parts and machine tools due to its good machinability, excellent formability, and low cost. However, some of its properties such as wear resistance, hardness, and corrosion resistance are inferior leading to poor tribological behavior. In order to enhance the tribological properties, surface modification is therefore necessary.

Thermochemical surface treatment is a surface modification technique in which a material surface is hardened by diffusing alien atoms into the surface. The

thermochemical surface treatment techniques are such as carburizing, carbonitriding, nitrocarburizing, and nitriding. Nitrocarburizing, consisting of diffusing nitrogen and carbon into the surface of ferrous materials, is a surface hardening technique for improving hardness and wear resistance (Liu & Yan, 2010; Wang *et al.*, 2015). The surface of nitrocarburized steels usually consists of a white layer and a diffusion zone. The white layer is composed of the  $\epsilon$ -Fe<sub>2.3</sub>[N.C] and  $\gamma'$ -Fe<sub>4</sub>N phases, providing low friction and high wear resistance. While the diffusion zone is mainly composed of  $\gamma'$ -Fe<sub>4</sub>N and  $\alpha''$ -Fe<sub>16</sub>N<sub>2</sub> phases. In the case of alloy steels, the nitride of the alloying elements is commonly found (Jacquet, Coudert, & Lourdin, 2011).

Prior to a surface treatment, a material surface preparation, such as cleaning, texturing, and pre-treating, may be done and can affect the material performance after the

---

\*Corresponding author  
Email address: prasert.a@sut.ac.th

surface treatment. A previous study reported that an initial surface roughness of a stainless steel had a significant effect on the surface morphology and properties of the steel after plasma nitriding (Li *et al.*, 2017). Furthermore, it has been reported that a smaller diffusion zone was formed in the samples with a high initial surface roughness (Singh *et al.*, 2006). This was attributed to an impediment of the nitrogen diffusion into the material surface caused by the austenite phase in stainless steel. Even though the effect of surface roughness on surface treated stainless steels has been investigated, there is a lack of study of such effect on surface treated low alloyed steels. Unfortunately, tribological study, such as wear and scratch tests, of the nitrocarburized low-alloyed steels have not been reported yet.

Some researchers have studied the effect of the pre-process roughness on coating characteristics and morphology after nitriding and nitrocarburizing processes (Cisquini *et al.*, 2019; Fathallah, Dakhli, & Terres, 2019; Terres, Fathallah, & Ghanem, 2017). However, there has been a lack of studying the effect of material surface roughness on tribological properties of the coated materials, in particular, wear. Understanding the effect of material roughness is also essential for industry aiming to improve coating quality. Therefore, the aim of this paper is to present the effect of surface roughness achieved by a surface preparation prior to the gas nitrocarburizing on the surface properties of gas nitrocarburized steels. Surface characterizations, such as surface roughness, microstructure, X-ray diffraction, microhardness, scratch test, and wear volume loss, were evaluated and discussed.

## 2. Materials and Methods

### 2.1 Material and sample preparation

The materials used in this study were AISI 1015 and AISI 4115 steels with chemical compositions (wt %) as C-0.15, Cr-0.092, Mn-0.45, Fe-balance of AISI 1015 and C-0.14, Cr-0.920, Mn-0.83, Fe-balance of AISI 4115. As-received steel rods with a diameter of 30 mm were normalized at 930 °C for 90 minutes. Then, they were cut into a circular disk shape with a thickness of 7 mm. The surface finish of the disk samples was achieved by two different methods: polishing and machining. The polished sample was prepared by polishing using a 2000-grade sandpaper prior to a fine polishing step using 1- $\mu\text{m}$  alumina. While, the machined sample was prepared by lathing at a spindle speed of 1600 rpm and a feed rate of 30 mm/min. The surface morphologies of specimens after surface preparation are shown in Figure 1.

Surface roughnesses were measured by Stylus Profilometer (Mitutoyo SurfTest SV-400) with a velocity of 0.5 mm/s and a length of 4.8 mm. An average initial surface roughness ( $R_a$ ) of the polished and machined samples before gas nitrocarburizing were  $0.027 \pm 0.004 \mu\text{m}$  and  $1.462 \pm 0.158 \mu\text{m}$ , respectively.

Prior to the gas nitrocarburizing process, the samples were wiped with alcohol and air-dried. Gas nitrocarburizing was carried out in a commercial heat treatment furnace (Koyo thermos system: ERT-304828-NFV) at 570 °C for 3 hours. The ambient gasses were ammonia ( $\text{NH}_3$ ) and Rx gas ( $\text{C}_3\text{H}_8:7.5\text{H}_2:2.5\text{N}_2$ ) flown into the furnace at a flow rate of 10  $\text{m}^3/\text{h}$ . In a final step, the samples were quenched in oil at 100°C.

### 2.2 Microstructure, crystalline structure, hardness, and tribological properties

To study microstructures of treated samples, a cross-section of the treated sample etched by 5% v/v nitric acid and rinsed with distilled water was observed using an optical microscope (OM, Nikon MM400). The thickness of a white layer was determined by taking an average thickness value measured from six different positions on a sample and three samples for each condition.

An examination of crystalline structures in the surface of the untreated and treated samples were performed using an X-ray diffractometer (Bruker D8 Advance). The crystalline phase characterization was carried out at 40 kV and 40 mA using a copper (Cu) tube as an anode with a wavelength of 1.5418 Å, an angle range of 35-50°, and an interval step of 0.02°.

Microhardness testing was carried out at an indentation load of 300 g for 10 s and 50 g for 10 s for case and core hardnesses, respectively. Measurement was performed on at least three samples for each condition and repeated at least three times on each sample. A case depth was determined in accordance with DIN 50190-3, and can be defined as a distance from the surface of nitrocarburizing layer to the point where the hardness limit is 50 HV above the core hardness which is equal to 250 HV for this study.

To determine the failure limit of the nitrocarburizing coating and evaluate the cohesion between coating and substrate, a scratch test was performed using a CSM Revetest® scratch tester equipped with an acoustic emission (AE) sensor. Cohesive strength was tested with a Rockwell-C diamond tip (200  $\mu\text{m}$  radius). The diamond tip was driven above the surface without lubrication to produce a scratch. The normal load on the diamond tip was increased linearly with time to induce a shear force on the surface. At the start of

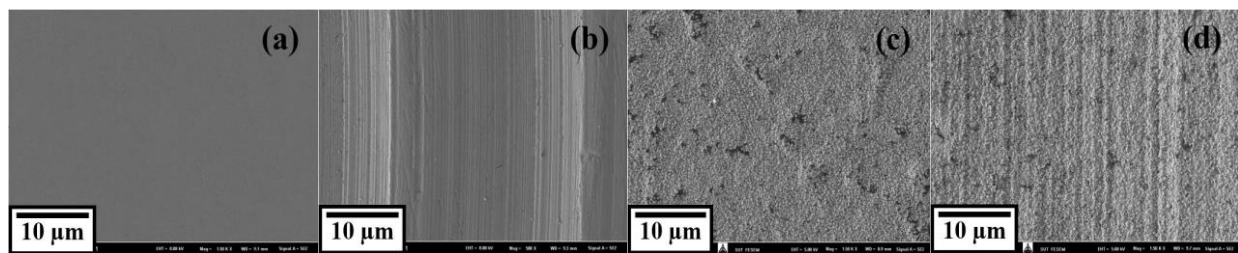


Figure 1. SEM images of the surface morphologies for (a) polished sample, (b) machined sample before gas nitrocarburizing; and for (c) polished sample, (d) machined sample after gas nitrocarburizing

a scratch test, a preload of 1 N was applied, then the applied load was continually increased at a loading rate of 100 N/min up until reaching a nominal maximum load of 100 N. The diamond tip was moving at a speed of 5 mm/min and the total scratch length was 4.95 mm.

Wear tests were performed on a pin-on-disk tribometer (Anton Paar). In the pin-on-disk test, a nitrocarburized sample, used as a disk specimen, was rotated against a 6-mm diameter ball specimen made of Al<sub>2</sub>O<sub>3</sub>. A contact load of 5 N was applied. The test was carried out at a sliding speed of 200 mm/min and radius (r) = 5 mm with a total sliding distance of 500 meter. After the wear test, a profile the wear track was obtained using an optical laser scanner (Zeiss SmartProof5). The wear volume loss can be calculated by multiplying an area loss determined from the cross-section profile image (Figure 2) by measuring the area. The wear volume loss (V) can be evaluated by multiplying the area loss (A) by the circumferential length of the wear track (2πr). The area loss was determined from the cross-section profile image (Figure 2) by measuring the area of material removed from the surface (A<sub>1</sub>) and subtracting A<sub>1</sub> by the areas of plastically deformed material (A<sub>2</sub> + A<sub>3</sub>). Thus, the wear volume loss (V) can be written as,  $V = A \times 2\pi r = (A_1 - (A_2 + A_3)) \times 2\pi r$ .

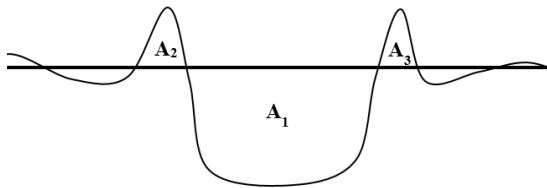


Figure 2. Cross sectional view of scratches obtained from optical laser scanner (Zeiss SmartProof5).

### 3. Results and Discussion

#### 3.1 Microstructure

In Figure 3, a white layer forming during nitrocarburizing process was observed on both polished and machined samples. Microstructure underneath the white layer mainly consisted of ferrite and pearlite. The average thickness of the white layer of the polished and machined samples were 17.52 and 16.19 μm, respectively for AISI 1015 steel, and were 12.43 and 12.71 μm, respectively for AISI 4115 steel. Even though the white layer thickness was not significantly influenced by the initial surface roughness, the Cr content in the steels has a substantial effect on the white layer thickness,

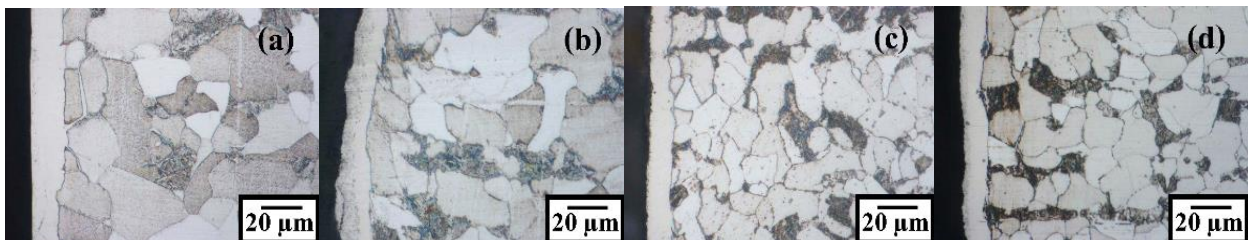


Figure 3. Optical micrographs of cross-section after gas nitrocarburizing (a) Polished AISI 1015 steel, (b) Machined AISI 1015 steel, (c) Polished AISI 4115 steel, and (d) Machined AISI 4115 steel

i.e., the samples made of AISI 1015 steel with a lower Cr content has a thicker white layer than those made of AISI 4115 steel with a higher Cr content.

During nitrocarburizing process, nitrogen and carbon atoms diffuse into the surface of steels. At the surface, a formation of a compound layer, often called white layer, primarily consisting of iron carbonitrides ( $\epsilon$ -Fe<sub>2.3</sub>[N.C] and  $\gamma'$ -Fe<sub>4</sub>N) phases took place. While, underneath the white layer, there is a formation of a diffusion layer where the diffusing nitrogen and carbon are dissolved interstitially in the ferritic matrix. The diffusion of nitrogen and carbon atoms generally depends on many factors such as process parameters and chemical compositions of the base material. Chromium was found to facilitate nitrogen diffusion into the steel (Holm & Spröge, 2018). With a higher Cr content, nitrogen tends to diffuse deeper into the core of the steel. Moreover, as nitrogen diffusion is enhanced, nitrogen concentration in the area near the surface is low, and therefore, a white layer formed becomes thinner.

In addition, a non-uniformity of the white layer formation on the machined samples was observed, i.e., the white layer is thicker in the hilltop area and thinner in the valley area (Figure 4). The observation in this study is in agreement with a previous work (Ebrahimi, Mahboubi, & Naimi-Jamal, 2015). It is likely that in an open area on the hilltop, nitrogen and carbon atoms have high mobility and can diffuse faster into the surface. However, in the valley area, the mobility of nitrogen and carbon atoms is limited leading to retarding of the white layer formation in the valley area.

In Figure 5, it is observed that the white layer produced was substantially porous, especially near the outer surface. To estimate the percentage of porosities per area, an image taken by SEM were converted into a binary image in which porosities, being less reflective areas, were shown in black while smooth and more reflective areas were shown in white. The percentage of porosities per area was then calculated from a ratio between the number of black pixels and the total number of black and white pixels. The percentage of porosities per area of the polished samples are 3.02% and 1.62% for AISI 1015 and AISI 4115, respectively; while in case of the machined samples they are 10.05% and 6.44% for AISI 1015 and AISI 4115, respectively.

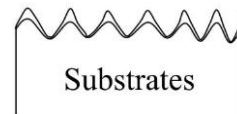


Figure 4. Schematic illustration of the white layer growth on rough surface

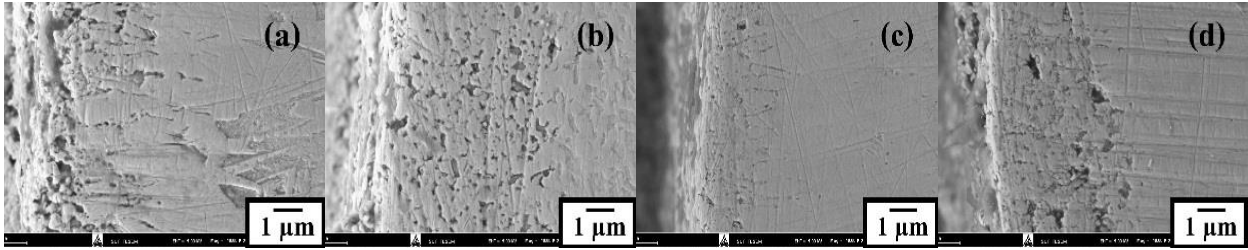


Figure 5. SEM images of cross-section of the outmost surface after gas nitrocarburizing (a) Polished AISI 1015 steel, (b) Machined AISI 1015 steel, (c) Polished AISI 4115 steel, and (d) Machined AISI 4115 steel

The amount of porosities occurring in the white layer was influenced by both the initial surface roughness and the chromium content. Although the effect of the initial roughness on the thickness of the white layer is unlikely, a white layer forming on a smooth surface of the polished samples is denser than that forming on a rough surface of the machined samples. This is attributed to an increase of a diffusion rate for samples with a rougher surface due to a relatively greater surface area, i.e., the rougher the surface, the faster the diffusion of nitrogen atoms into the steel. With a high diffusion rate, a number of nitrogen and carbon atoms tend to diffuse into the steel core rather than remain in the steel surface while the white layer is forming. The diffusion therefore results in generation of a large amount of voids in the white layer.

The white layer forming on the surface of AISI 4115 steel with higher chromium content tends to be thin and dense, while the white layer forming on the surface of AISI 1015 steel with lower chromium content is thick and porous. This finding is in agreement with a previous study reported that porosity was affected by the thickness of the white layer (Karakan, Alsaran, & Çelik, 2004).

### 3.2 Surface roughness

The average surface roughness ( $R_a$ ) results before and after gas nitrocarburizing is shown in Figure 6. The results indicate an increase of the roughness after gas nitrocarburizing for the polished samples. In Figure 1(c), a rough surface of a white layer forming on top of the polished steel surface can be observed. An increase of roughness due to a rough white layer is in agreement with the previous study (Aghajani, Torshizi, & Soltanieh, 2017). However, as the roughness of the machined samples was relatively high, the rough surface of the white layer does not significantly affect the overall surface roughness of the machined samples after nitrocarburizing.

For polished samples, roughness of AISI 1015 is higher than those of AISI 4115. This is due to the nature of microstructure development of a white layer which results in an uneven morphology on a surface. As the white layer thickness increases, the more pronounced effect on the roughness can be observed. Therefore, a thick white layer forming on the polished AISI 1015 steel tends to be rougher than a thin white layer forming on the polished AISI 4115 steel.

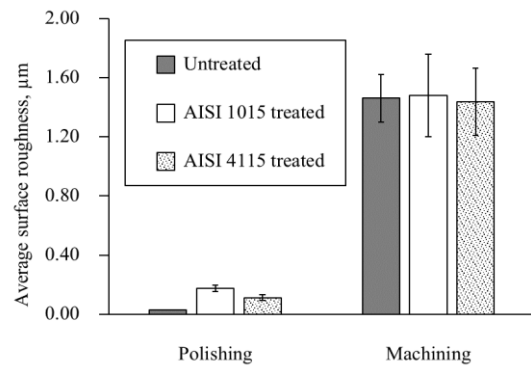


Figure 6. Average surface roughness of the two different surface states of both steels before and after gas nitrocarburizing

### 3.3 XRD

The XRD result of the polished sample before the heat treatment reveals the highest intensity of ferrite comparing to machined sample (Figure 7). It is likely that the roughness has an effect on the incidence and diffraction of X-ray during the XRD analysis, therefore a clear peak of ferrite can be observed in the case of a polished surface.

During nitrocarburizing, a white layer consisting of two phases,  $\epsilon$ -Fe<sub>2-3</sub>[N.C] and  $\gamma'$ -Fe<sub>4</sub>N, has formed. At the start of nitrocarburizing, due to a relatively higher transferring rate of carbon, a carbon-rich layer, cementite ( $\theta$ ), firstly forms. The  $\epsilon$ -phase develops subsequently as nitrogen atoms starts to diffuse into ferrite, followed by a conversion of  $\theta$ -phase into  $\epsilon$ -phase until a single-phase  $\epsilon$  layer results. Due to limited solubility of carbon in ferrite, a carbon-poor phase,  $\gamma'$ , then develops as diffusion of nitrogen atoms increases, resulting in an  $\epsilon$ -Fe<sub>2-3</sub>[N.C] +  $\gamma'$ -Fe<sub>4</sub>N compound layer.

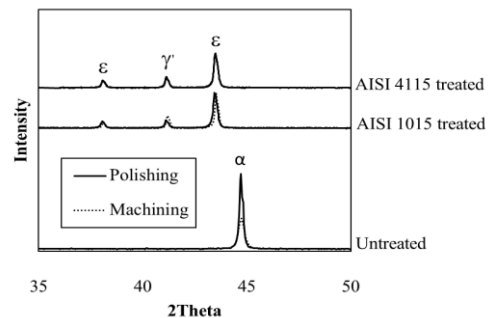


Figure 7. X-ray diffraction patterns of the untreated and treated samples with two different surface states of both steels

The XRD results in Figure 7 indicate the formation of a white layer consisting of two phases,  $\epsilon$ -Fe<sub>2.3</sub>[N.C] and  $\gamma'$ -Fe<sub>4</sub>N, for the treated samples. With a higher surface roughness, a machined surface results in larger actual surface area. Therefore, a faster rate of a white layer formation on a machined surface is likely due to an increase in diffusion rate of nitrogen atoms into the surface. Since the formation of a white layer occur at a faster rate, the development of  $\gamma'$  phase on a rough sample will start earlier than that on a polished surface.

**3.4 Hardness**

The hardness results of specimens after gas nitrocarburizing are shown in Figure 8. It can be seen that the surface hardness of the machined samples was slightly lower than the polished ones for the same steel. The decrease of the surface hardness was affected by the porosity underneath the surface (Figure 5) as discussed previously.

Treated AISI 4115 steel has a higher surface hardness than treated AISI 1015 steel because of the Cr content in the AISI 4115 (Holm & Sproge, 2018). The AISI 4115 steel with a relatively high Cr content affects the nitrogen diffusion and leads to the formation of chromium nitride which has high hardness.

The AISI 1015 hardness profiles were rapidly decreased right underneath the surface. While, the AISI 4115 hardness profiles were gradually decreased. This is attributed to alloying elements in the steels (Jacquet *et al.*, 2011). Cr content in AISI 4115 increases nitrogen solubility in ferrite and results in substantial nitrogen diffuses into the substrate. However, the depths of the diffusion zone or case depths of samples with different surface preparations were not different indicating that the surface roughness did not significantly affect the diffusion distance of nitrogen atoms into the substrate.

**3.5 Scratch test**

Figure 9 shows scratch tracks and acoustic emission signal peaks for both steels at an applied load of 52 N. From

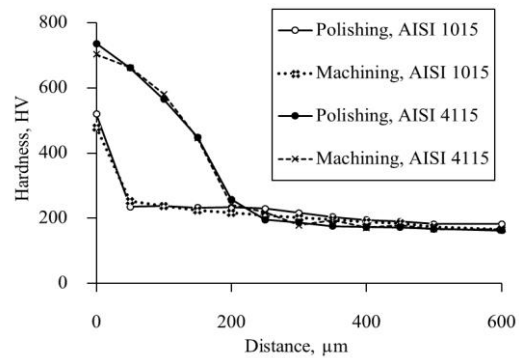


Figure 8. Hardness profiles of the two different surface states of both steels from the surface to substrates after gas nitrocarburizing

Figure 9(a), Chevron cracking and chipping failure were observed on the AISI 1015 sample. The acoustic emission signal of the AISI 1015 sample revealed the highest peak at 70.3 N indicating that the surface damage started. The treated AISI 4115 had a higher cohesive strength than the treated AISI 1015. The cohesive failure at the surface can be related to the hardness profile (Jacquet *et al.*, 2011) as shown in Figure 8, where an abrupt drop in the hardness from surface to substrate was verified.

**3.6 Wear properties**

The friction coefficient versus distance curves of the nitrocarburized samples are shown in Figure 10. The friction coefficient of AISI 1015 rapidly approached a steady stage at 50 m (Figure 10(a)) because the low surface hardness led to faster wear in the first stage. The friction coefficients of AISI 4115 could be divided into three stages as observed in Figure 10(b). From 0 – 50 m, the friction coefficient abruptly increased because of the high contact pressure. After that, the contact pressure forces gradually decreased while the contact area increased. From 50 – 350 m, the surface failure occurred continuously from surface fatigue after testing for a long distance. From 350 – 500 m, a steady stage was reached

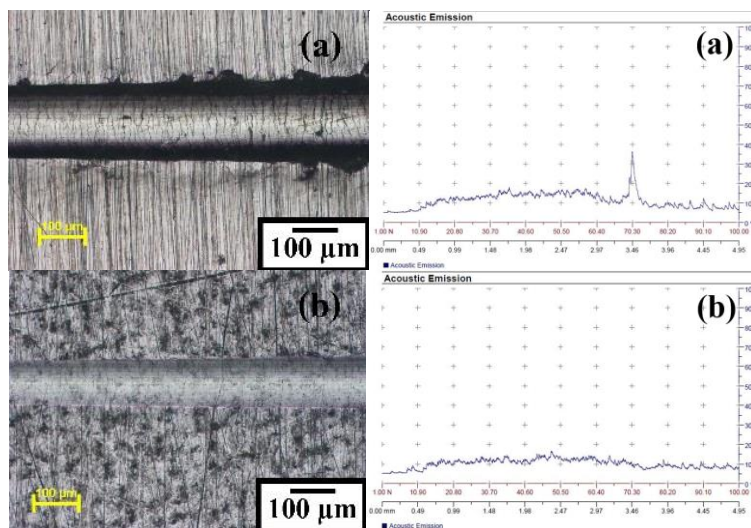


Figure 9. Scratch tracks at a load of 52 N after treated and acoustic emission signal peaks versus on (a) AISI 1015 steel and (b) AISI 4115 steel

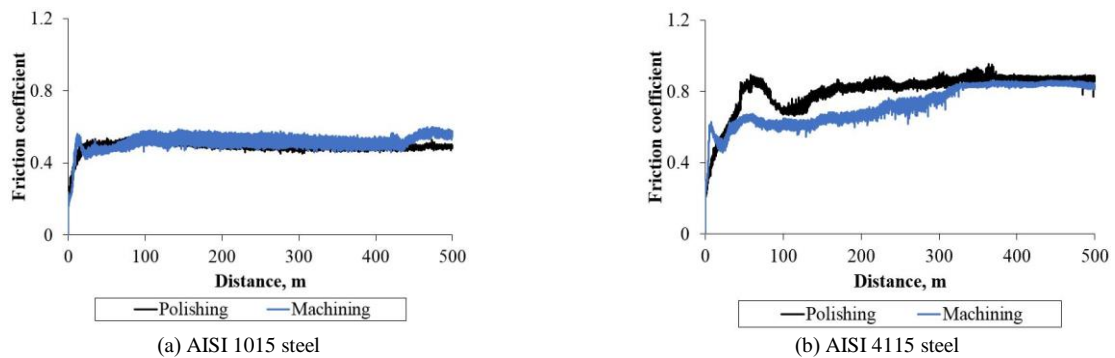


Figure 10. The variation of friction coefficient versus distance of the polished and machined samples (a) AISI 1015 steel, (b) AISI 4115 steel

because of constant contact pressure and abrasive wear (Jacquet *et al.*, 2011; Zeng, Yamaguchi, & Nishio, 2015). The average friction coefficients for AISI 1015 and AISI 4115 were 0.505 and 0.795, respectively. The AISI 4115 friction coefficient was higher than the AISI 1015 because of higher cohesive strength (Liu & Yan, 2010). However, the friction coefficient is also affected by other factors, such as surface roughness, wear mechanisms, microstructure hardness, white layer thickness and abrasive material.

The high surface roughness increased wear volume loss, when the alumina ball plowed the surface, causing a lot of debris to fall out. The sample with high surface roughness had many hills on the surface which tended to create more debris. The debris has high hardness thus it can lead to an increased wear (Liu & Yan, 2010; Wang *et al.*, 2015). Figure 12 confirm that the wear track width of the polishing sample is smaller the machining sample.

From Figure 11, the treated AISI 4115 had a higher wear volume loss the AISI 1015 due to the hard debris. The high hardness of debris increases wear volume loss resulting in increased abrasive wear (Jacquet *et al.*, 2011). The result was different from other previous works (Li *et al.*, 2017; Liu & Yan, 2010), due to abrasive material which ball plug on a dish during wear tests. The debris has damaged the sample or the abrasive material. In this study, the hardness of samples was lower than the abrasive material causing more severe damage on the samples. The results of the wear test demonstrate that nitrocarburized AISI 1015 sample with low surface roughness could produce an appropriate white layer to improve wear resistance.

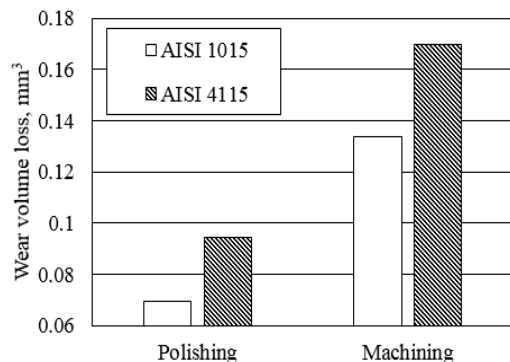


Figure 11. Wear volume loss results

#### 4. Conclusions

Gas nitrocarburizing was conducted on the surface of AISI 1015 steel and AISI 4115 steel. The depth of the diffusion zone decreases with increasing of Cr element. The phases of the white layer mainly consist of  $\epsilon$ -Fe<sub>2-3</sub>[N.C] and  $\gamma$ '-Fe<sub>4</sub>N. The surface hardness of the treated AISI 4115 was approximately 700 – 810 HV which was higher than the treated AISI 1015 steel due to the different chemical compositions such as Cr element. The Cr element improves surface hardening performance and facilitates nitrogen and carbon diffusions into the substrate.

The cohesive strength of both steels depends on the different cohesion of the surface and the substrates. The treated AISI 4115 has higher cohesion than the treated AISI 1015 due to the hardness profile. The AISI 4115 hardness gradually decreased from surface to substrate, while, the AISI 1015 hardness abruptly decreases. The wear volume loss increased with an increase of the surface roughness, while the sample with higher surface roughness produced more debris during the wear test.

#### Acknowledgements

The authors are grateful for the financial support for this study provided by Suranaree University of Technology and The Center for Scientific and Technological Equipment, Suranaree University of Technology, Mechanical laboratory of Thammasat University and Thai Tohken Thermo Co.,Ltd.

#### References

- Aghajani, H., Torshizi, M., & Soltanieh, M. (2017). A new model for growth mechanism of nitride layers in plasma nitriding of AISI H11 hot work tool steel. *Vacuum*, 141, 97-102.
- Cisquini, P., Ramos, S. V., Viana, P. R. P., Lins, V. d. F. C., Franco Jr, A. R., & Vieira, E. A. (2019). Effect of the roughness produced by plasma nitrocarburizing on corrosion resistance of AISI 304 austenitic stainless steel. *Journal of Materials Research and Technology*, 8(2), 1897-1906.
- Ebrahimi, M., Mahboubi, F., & Naimi-Jamal, M. R. (2015). Wear behavior of DLC film on plasma nitrocarburized AISI 4140 steel by pulsed DC PACVD: effect of nitrocarburizing temperature. *Diamond and Related Materials*, 52, 32-37.

- Fathallah, B. B., Dakhli, C. E., & Terres, M. A. (2019). The effect of grinding parameters and gas nitriding depth on the grindability and surface integrity of AISI D2 tool steel. *The International Journal of Advanced Manufacturing Technology*, 104(1-4), 1449-1459.
- Holm, T., & Sproge, L. (2018). Furnace atmospheres 3, Nitriding and Nitrocarburizing. *AGA Report GIM*, 89267.
- Jacquet, P., Coudert, J., & Lourdin, P. (2011). How different steel grades react to a salt bath nitrocarburizing and post-oxidation process: Influence of alloying elements. *Surface and Coatings Technology*, 205 (16), 4064-4067.
- Karakan, M., Alasaran, A., & Çelik, A. (2004). Effect of process time on structural and tribological properties of ferritic plasma nitrocarburized AISI 4140 steel. *Materials and design*, 25(4), 349-353.
- Li, Y., He, Y., Xiu, J., Wang, W., Zhu, Y., & Hu, B. (2017). Wear and corrosion properties of AISI 420 martensitic stainless steel treated by active screen plasma nitriding. *Surface and Coatings Technology*, 329, 184-192.
- Liu, R. L., & Yan, M. F. (2010). Improvement of wear and corrosion resistances of 17-4PH stainless steel by plasma nitrocarburizing. *Materials and Design (1980-2015)*, 31(5), 2355-2359.
- Singh, G. P., Alphonsa, J., Barhai, P., Rayjada, P., Raole, P., & Mukherjee, S. (2006). Effect of surface roughness on the properties of the layer formed on AISI 304 stainless steel after plasma nitriding. *Surface and Coatings Technology*, 200(20-21), 5807-5811.
- Terres, M. A., Fathallah, B. B., & Ghanem, A. (2017). Effects of surface pre-treatment on the Nitrided layers properties. *American Journal of Mechanical and Industrial Engineering*, 2(1), 41-47.
- Wang, Y., Yan, M., Li, B., Guo, L., Zhang, C., Zhang, Y., Li, R. (2015). Surface properties of low alloy steel treated by plasma nitrocarburizing prior to laser quenching process. *Optics and Laser Technology*, 67, 57-64.
- Zeng, X., Yamaguchi, T., & Nishio, K. (2015). Surface nitrocarburizing of Ti-6Al-4 V alloy by YAG laser irradiation. *Surface and Coatings Technology*, 262, 1-8.